J|A|C|S
ARTICLES
Published on Web 03/05/2004

Competitive Paths for Methanol Decomposition on Pt(111)

Jeff Greeley and Manos Mavrikakis*

Contribution from the Department of Chemical and Biological Engineering, University of Wisconsin-Madison, Madison, Wisconsin 53706

Received August 1, 2003; E-mail: manos@engr.wisc.edu

Abstract: Periodic, self-consistent, Density Functional Theory (PW91-GGA) calculations are used to study competitive paths for the decomposition of methanol on Pt(111). Pathways proceeding through initial C−H and C−O bond scission events in methanol are considered, and the results are compared to data for a pathway proceeding through an initial O−H scission event [Greeley et al. *J. Am. Chem. Soc.* **2002**, *124*, 7193]. The DFT results suggest that methanol decomposition via CH_2OH and either formaldehyde or HCOH intermediates is an energetically feasible pathway; O−H scission to CH_3O, followed by sequential dehydrogenation, may be another realistic route. Microkinetic modeling based on the first-principles results shows that, under realistic reaction conditions, C−H scission in methanol is the initial decomposition step with the highest net rate. The elementary steps of all reaction pathways (with the exception of C−O scission) follow a linear correlation between the transition state and final state energies. Simulated HREELS spectra of the intermediates show good agreement with available experimental data, and HREELS spectra of experimentally elusive reaction intermediates are predicted.

Introduction

The reaction of methanol on platinum has attracted great interest in recent years as the principal chemistry occurring on the anodes of direct methanol fuel cells (DMFCs), and excellent reviews describing the behavior of liquid-phase chemistry in DMFCs exist.[1−4] DMFCs offer the prospect of direct conversion of methanol to electricity with efficiencies substantially larger than those obtained with conventional, combustion-based power generation systems. The perfomance of DMFCs, however, is limited, among other factors, by CO poisoning of the anode surface. This poisoning is acute for pure platinum anodes.

Another reaction process that has given impetus to the study of methanol on platinum is known as Aqueous Carbohydrate Reforming (ACR). In this process, hydrogen is produced from aqueous reforming of sugars over platinum.[5] Methanol provides a good model system for understanding specific aspects of this process because, although it is a small molecule, it possesses many of the chemical characteristics of more complex carbohydrates.

Many studies of methanol decomposition processes have focused on *liquid-phase* DMFC chemistry.[6−8] These studies have yielded a number of interesting conclusions; for example, Franaszczuk et al.[6] demonstrated that the initial step in liquid-phase methanol decomposition involves the scission of a C−H bond. Numerous analyses have also dealt with *vapor-phase* chemistry in both high-pressure and ultrahigh vacuum (UHV) conditions;[9] these vapor-phase conditions are more amenable to highly controlled studies, and they may also be quite relevant to practical DMFC use since vapor-phase DMFC's permit easier access of fuel to the anode[1].

The present work is directly relevant to methanol decomposition on platinum under UHV conditions; the study enhances and completes our original analysis of methanol decomposition on Pt(111).[10] Details of existing *experimental* studies of this reaction can be found in our original article. *Theoretical* studies of the thermochemistry[11,12] and kinetics[13,14] of the reaction have tentatively suggested that methanol decomposition to CO and H_2 proceeds through an initial C−H bond scission to produce hydroxymethyl (CH_2OH). The adsorption of other intermediates (formaldehyde[15,16] and formyl[17]) in the methanol decomposition pathway has been studied separately using extended Hückel and DFT calculations, but to our knowledge, no study of the decomposition barriers of these species exists.

In this article, we present a systematic periodic, self-consistent, Density Functional Theory study of the two methanol

(1) Hamnett, A. *Catal. Today* **1997**, *38*, 445−457.
(2) Williams, K.; Burstein, T. *Catal. Today* **1997**, *38*, 401−410.
(3) Burstein, G.; Barnett, C.; Kucernak, A.; Williams, K. *Catal. Today* **1997**, *38*, 425−437.
(4) Beden, B.; Lamy, C.; Leger, J. R. *Electrocatalytic Oxidation of Oxygenated Aliphatic Organic Compounds at Noble Metal Electrodes*; Bockris, J. O. M., Conway, B. E., White, R. E., Eds.; Plenum Publishers: New York, 1992; Vol. 22, 566 pages.
(5) Cortright, R. D.; Davda, R. R.; Dumesic, J. A. *Nature* **2002**, *418*, 964−967.
(6) Franaszczuk, K.; Herrero, E.; Zelenay, P.; Wieckowski, A.; Wang, J.; Masel, R. I. *J. Phys. Chem.* **1992**, *96*, 8509−8516.
(7) Lu, G. Q.; Chrzanowski, W.; Wieckowski, A. *J. Phys. Chem. B* **2000**, *104*, 5566−5572.
(8) Sriramulu, S.; Jarvi, T. D.; Stuve, E. M. *J. Electronanal. Chem.* **1999**, *467*, 132−142.
(9) Jarvi, T. D.; Stuve, E. M. Fundamental Aspects of Vacuum and Electrocatalytic Reactions of Methanol and Formic Acid on Platinum Surfaces; Lipkowski, J., Ross, P. N., Eds.; Wiley-VCH: New York, 1998; 376 pages.
(10) Greeley, J.; Mavrikakis, M. *J. Am. Chem. Soc.* **2002**, *124*, 7193−7201.
(11) Kua, J.; Goddard, W. *J. Am. Chem. Soc.* **1999**, *121*, 10928−10941.
(12) Ishikawa, Y.; Liao, M.; Cabrera, C. *Surf. Sci.* **2000**, *463*, 66−80.
(13) Desai, S. K.; Neurock, M.; Kourtakis, K. *J. Phys. Chem. B* **2002**, *106*, 2559−2568.
(14) Greeley, J.; Nørskov, J. K.; Mavrikakis, M. *Ann. Rev. Phys. Chem.* **2002**, *53*, 319−348.
(15) Delbecq, F.; Sautet, P. *Langmuir* **1993**, *9*, 197−207.
(16) Delbecq, F.; Sautet, P. *Surf. Sci.* **2002**, *211*, 398−406.

10.1021/ja037700z CCC: $27.50

Table 1. Selected Geometric and Energetic Parameters for Intermediates Resulting from Methanol Decomposition on Pt(111)

species	binding energy (eV)	binding configuration	bond length (Å)	angle (wrt surf. normal – degrees)	X-Pt bond length (Å)	$\Delta\varphi$ upon adsorption (eV)
methanol (CH_3OH)	−0.33	top−bound through oxygen	1.44[a]	63[d]	2.43[h]	−1.08
methoxy (CH_3O)	−1.54	top−bound through oxygen	1.40[a]	59[d]	2.03[h]	−0.44
formaldehyde (CH_2O)	−0.50	top-bridge-top−bound through oxygen and carbon	1.34[a]	88[d]	2.10[h]	−0.21
					2.17[g]	
formyl (CHO)	−2.36	top−bound through carbon	1.21[a]	144[d]	2.02[g]	−0.05
carbon monoxide (CO)	−1.82	fcc−bound through carbon	1.20[a]	180[d]	2.13[g]	0.43
hydroxymethyl (H_2COH)	−1.98	top−bound through carbon	1.38[a]	66[d]	2.14[g]	−0.47
hydroxymethylene (HCOH)	−3.24	bridge−bound through carbon	1.34[a]	45[d]	2.13[g]	−0.26
hydroxymethylidyne (COH)	−4.45	fcc−bound through carbon	1.33[a]	0[d]	2.04[g]	−0.71
methyl (CH_3)	−1.93	top−bound through carbon	1.10[b]	72[e]	2.11[g]	−0.44
hydroxyl (OH)	−2.12	tilted top−bound through oxygen	0.99[c]	72[f]	2.02[h]	0.08
hydrogen (H)	−2.71	top−but fcc is nearly degenerate			1.57[i]	−0.09

[a] O−C BL. [b]C−H BL. [c]O−H BL. [d]O−C angle. [e]C−H angle. [f]O−H angle. [g]C−Pt. [h]O−Pt. [i]H−Pt. φ = workfunction.

decomposition pathways on Pt(111) starting with either C−H or C−O bond scission. We address both the thermochemistry and the reaction barriers of the elementary reaction steps in these pathways, and we present a detailed potential energy surface showing the interconversions of the various intermediates in the pathways. In addition, we report calculated vibrational frequencies for the adsorbed states of these intermediates, and we correlate the energies of the transition states with the energies of the final states for all elementary steps in the reaction network. Finally, by using a microkinetic model to assist in the interpretation of our DFT data, we draw conclusions about the likely decomposition mechanism of methanol on Pt(111).

Methods

DACAPO, the total energy calculation code,[18] is used for all calculations in this study. Details of the calculations can be found in a previous publication.[10]

Vibrational frequencies are calculated on two-layer slabs (we find only minor differences from frequencies calculated on 3-layer slabs) by numerical differentiation of the forces using a second-order finite difference approach with a step size of 0.015 Å.[19] The resulting Hessian matrix is then mass-weighted and diagonalized to yield the frequencies and normal modes of the system. For gas-phase methanol, this approach yields frequencies with an average deviation of 48 cm^{-1} from experiment. Zero-point energies (ZPEs) are calculated from the frequencies; the ZPE's are only included in the results, however, where explicitly specified. Specular HREELS intensities are estimated from the spatial derivatives of the component of the dipole moment perpendicular to the slabs; these derivatives are calculated with the same numerical scheme as is used for the force derivatives.

The minimum energy reaction paths of various elementary steps are studied using the Climbing Image Nudged Elastic Band (CINEB) method.[20−23] Although this approach does not employ frequency analyses (see, for example, the ACS Symposium Series[24] for a detailed description of these analyses), the mathematics of the technique are well-defined,[23,25] and it has been shown to give excellent convergence to saddle points on analytical potential energy surfaces. In addition, we have found in the present work that, when harmonic frequencies are calculated for NEB-optimized transition states, only a single imaginary frequency is obtained in nearly all cases. This fact is further evidence that the transition states found with the NEB algorithm are true saddle points on the potential energy surface.

Results

Structure and Adsorption Thermochemistry of Reaction Intermediates. Geometric and energetic information for the most favorable configurations of methanol and of intermediates resulting from methanol decomposition through an initial *O−H bond scission* on Pt(111) is given in the first five entries of Table 1 (see our previous publication for a detailed discussion).[10] Data for atomic hydrogen are given in the last entry of this table; we note that hydrogen has no strong site preferences on Pt(111). Not shown in the table is information about a methanol configuration that, while higher in energy than the most favorable methanol configuration, is relevant for methanol decomposition through an initial C−H scission (see description in "Reaction Barriers of Elementary Steps" section). The configuration is similar to the state in Table 1, but with the methyl group rotated such that a single carbonic hydrogen points toward the surface. This hydrogen sits 2.62 Å above the surface plane, and the binding energy (BE) of the methanol configuration is −0.24 eV.

Schematics of the most stable state of each reaction intermediate resulting from methanol decomposition starting with *C−H bond scission*, together with a definition of appropriate bond angles, can be found in Figure 1a (see Table 1 for a summary of energetic and geometric information).[26] Similar data for the products of C−O scission in methanol are presented in Figure 1b (see also Table 1).

Vibrational Frequencies of Surface Reaction Intermediates. Vibrational frequencies for all stable intermediates resulting from C−H and O−H bond scission in methanol are given in Table 2; the details of the calculated vibrational spectra are analyzed, for selected adsorbates, in the Discussion section. For methanol itself, simulated HREEL spectra (assuming measurement of electrons at the specular angle), corresponding to oxygen-bound configurations with two (the most stable con-

(17) Gomes, J.; Gomes, J. *J. Electronanal. Chem.* **2000**, *483*, 180−187.
(18) Hammer, B.; Hansen, L. B.; Nørskov, J. K. *Phys. Rev. B* **1999**, *59*, 7413−7421.
(19) Greeley, J.; Mavrikakis, M. *Surf. Sci.* **2003**, *540*, 215−229.
(20) Ulitsky, A.; Elber, R. *J. Chem. Phys.* **1990**, *92*, 1510.
(21) Mills, G.; Jonsson, H.; Schenter, G. K. *Surf. Sci.* **1995**, *324*, 305.
(22) Henkelman, G.; Jónsson, H. *J. Chem. Phys.* **2000**, *113*, 9978−9985.
(23) Henkelman, G.; Uberuaga, B. P.; Jónsson, H. *J. Chem. Phys.* **2000**, *113*, 9901−9904.
(24) Truhlar, D. G.; Morokuma, K. *Transition State Modeling for Catalysis*; Oxford University Press: Washington, DC, 1999; Vol. 721.
(25) Henkelman, G.; Jónsson, H. *J. Chem. Phys.* **1999**, *111*, 7010−7022.

(26) Several other binding modes for all reaction intermediates have been studied, but these modes are less stable and have been omitted for brevity.

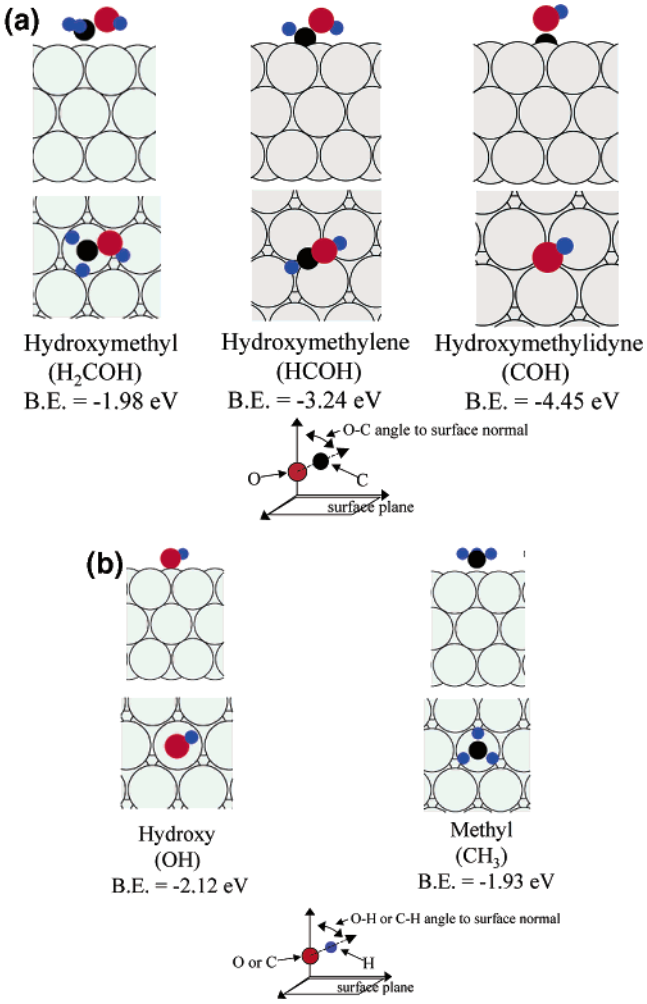

Figure 1. Cross-section and top view of (a) Most stable binding configurations for hydroxymethyl, hydroxymethylene, and hydroxymethylidyne on Pt(111) (b) Most stable binding configurations for hydroxyl and methyl on Pt(111). Zero point energies are not included.

figuration−first spectrum) and one (second spectrum) methyl hydrogen atoms pointing toward the surface, are provided in Figure 2a. For methoxy, frequencies are also given for two states (the most stable tilted state−top, and the most stable perpendicular state−fcc); simulated spectra for these configurations are given in Figure 2b. For CO, frequencies and spectra (Figure 2c) for two states (fcc and top) are presented. For the remaining intermediates, frequencies, and intensities are given in tabular form (Table 2) only.

Reaction Barriers of Elementary Steps. The reaction coordinate showing C−H bond scission in methanol, yielding adsorbed hydroxymethyl (CH_2OH) and atomic hydrogen, is given in Figure 3. The initial state of this pathway is the metastable methanol configuration described above. This configuration is 0.09 eV higher in energy than the most stable state, but it allows the carbonic hydrogen to begin the dissociation process closer to the Pt(111) surface, thereby giving a shorter dissociation pathway. The reaction coordinate begins with a C−H stretch vibration at 3067 cm^{-1} (Table 2; the frequency of this mode becomes imaginary at the transition state) and ends with CH_2OH bound through carbon at a top site and H adsorbed at an hcp site. The reaction barrier for this step is 0.67 eV, and the energy change of reaction is −0.16 eV (exothermic step).

Table 2. Calculated Vibrational Frequencies and Specular HREELS Intensities for Stable Intermediates in Methanol Decomposition on Pt(111)[a]

species	frequencies (cm^{-1})	intensities	species	frequencies (cm^{-1})	intensities
CH_3OH	3674	0.01	CH_3OH	3714	0.03
(O-bound,	3110	- -	(O-bound,	3101	- -
two carbonic	3045	0.05	one carbonic	3067	0.06
H's toward	2970	0.04	H toward	2989	0.05
surface)	1438	0.02	surface)	1444	- -
	1427	0.01		1426	0.02
	1416	- -		1419	0.05
	1294	0.03		1274	0.05
	1130	0.01		1133	0.01
	1043	0.07		1057	0.09
	976	0.32		961	0.51
	507	1.00			
CH_3O (tilted top)	2986	0.18	CH_3O (fcc perp.)	3062	- -
	2895	0.07		3049	0.01
	2818	0.01		2971	0.23
	1403	0.27		1425	0.01
	1380	0.01		1419	- -
	1367	- -		1401	0.05
	1090	0.03		1111	- -
	1086	0.07		1101	0.01
	1021	0.10		968	1.00
	431	1.00		257	- -
	256	- -			
CO (top)	2137	1.00	CO(fcc)	1822	1.00
	467	0.06		356	0.01
	383	- -		324	- -
	383	- -		313	- -
CH_2OH (top)	3688	0.01	CH_2O (top-	3001	0.01
	3117	- -	bridge-top)	2922	0.08
	2988	- -		1422	0.02
	1415	- -		1194	0.04
	1327	0.04		1125	- -
	1171	0.01		944	0.13
	1081	0.04		580	0.09
	1014	0.59		494	1.00
	735	0.06		325	0.08
	490	1.00			
	418	0.94			
	261	0.09			
HCOH (bridge)	3280	0.03	HCOH (top)	3110	0.18
	2994	- -		3050	0.03
	1329	0.10		1377	1.00
	1168	1.00		1365	0.32
	1122	0.23		1175	0.37
	856	- -		941	0.01
	472	- -		654	0.01
	453	- -		613	0.02
	323	- -		350	0.05
	307	0.04			
CHO (top)	2692	0.01	COH (fcc)	3704	0.05
	1785	- -		1292	0.32
	959	1.00		1100	1.00
	804	0.14		523	0.15
	491	0.96		503	0.01
	265	- -		385	0.02
CH_3OH (g)	3859	N/A			
	3086				
	3007				
	2954				
	1452				
	1442				
	1420				
	1315				
	1129				
	1051				
	1005				
	285				

[a] Only modes with frequencies of greater than 250 cm^{-1} are shown. All intensities are scaled by the intensity of the highest intensity mode. "N/A" for gas-phase methanol indicates that intensities were not calculated for this species, as the gas-phase transition rules differ from the corresponding rules on metallic surfaces. "- -" indicates a scaled intensity of less than 0.01.

The reaction pathways for C−H bond scission in hydroxymethyl (H−CHOH), hydroxyl hydrogen abstraction from hy-

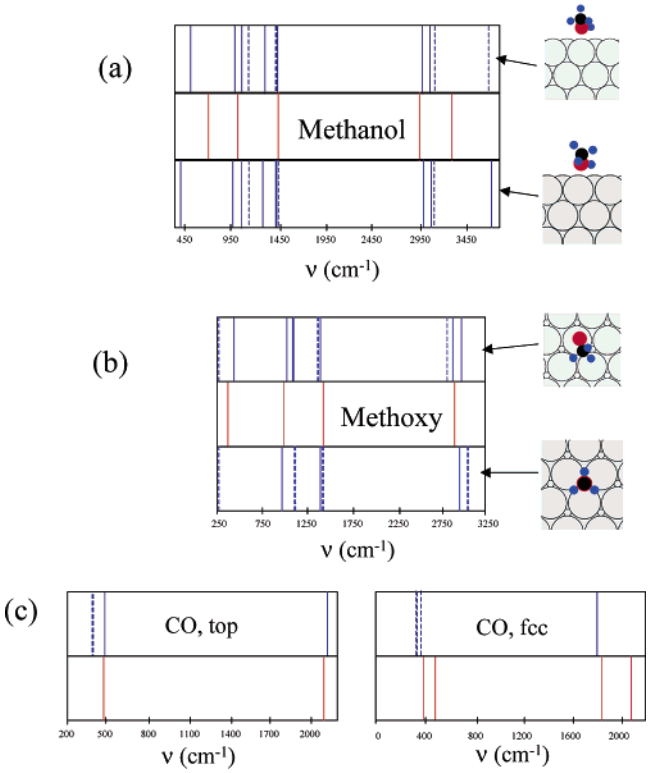

Figure 2. Simulated and experimental spectra for (a) *methanol*, (b) *methoxy*, and (c) *carbon monoxide* on Pt(111). Blue lines denote theoretical results, and red lines indicate experimental results. The topmost methanol spectrum corresponds to the most stable methanol configuration. The solid lines denote modes with relatively large calculated intensities while the dotted lines denote modes of lesser intensities. Insets show the calculated structures of methanol and methoxy; red circles denote O, black circles denote C, and blue circles indicate H. Experimental data are taken from Sexton[Sexton, B., *Surf. Sci.* **1981**, *102*, 271−281] (a,b) and Steininger et al.[Steininger et al., *Surf. Sci.* **1982**, *123*, 264−282] (c).

droxymethyl (CH_2O-H), and C−H scission in hydroxymethylene (H−COH), together with the associated energetics for each of these elementary steps, are summarized in Figure 4. The reaction coordinate for the H−CHOH step begins with a C−H stretch at 2988 cm^{-1} (Table 2) and ends with hydroxymethylene and atomic hydrogen adsorbed on adjacent top sites. CH_2O-H scission begins with an O−H stretch at 3688 cm^{-1} and ends with formaldehyde in a top-bridge-top configuration and hydrogen on an adjacent top site. Finally, H−COH scission begins with a C−H stretch at 2994 cm^{-1} and ends with COH bound through carbon at an fcc site and H adsorbed on a top site. All of the indicated vibrational modes become imaginary at the transition state.

The reaction coordinate for O−H bond scission in HCOH is shown in Figure 5. The process begins with an O−H stretch at 3280 cm^{-1} (Table 2, the frequency becomes imaginary at the TS). As the oxygen−hydrogen bond is broken, the H atom moves toward the top site of a neighboring platinum atom, and the remaining HCO group rotates in the same direction as the hydrogen. After the transition state is reached, however, the HCO group rotates in the opposite direction (away from the H atom). The final state in this pathway is a formyl-like complex although this state is not actually a true local minimum on the potential energy surface. Rather, it appears to be a saddle point; relaxation of all degrees of freedom of this state results in spontaneous C−H bond scission to produce CO (the point on

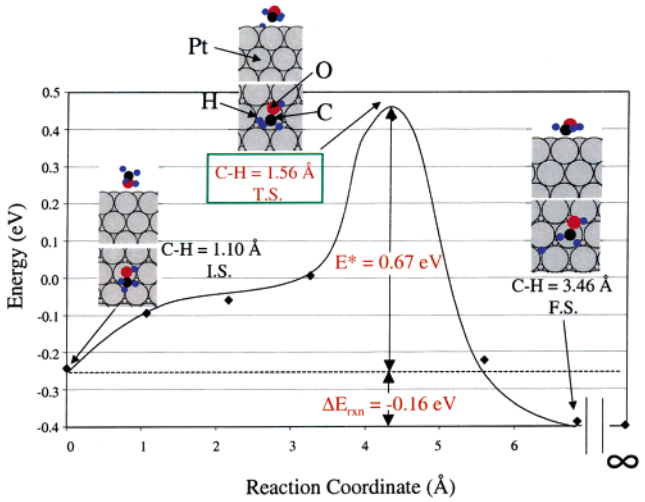

Figure 3. Reaction coordinate for C−H bond scission in *methanol* on Pt-(111). Insets provide cross-section and top views of IS (= initial state), TS (= transition state), and FS (= final state); the length of the bond being broken is indicated close to each inset. Oxygen, carbon, hydrogen, and platinum atoms are as indicated in the transition state inset. Zero point energies are not included. The line denoting the energy of the system is only a guide to the eye. The energy zero is gas-phase methanol and a clean Pt(111) slab at infinite separation from one another. The initial MeOH state of this pathway is 0.09 eV higher in energy than the most stable MeOH state; this configuration allows the carbonic hydrogen to begin the dissociation process closer to the Pt(111) surface, thereby facilitating dissociation.

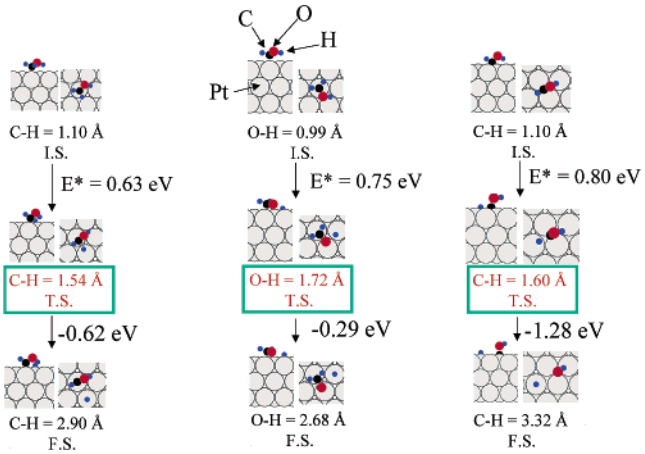

Figure 4. Reaction coordinates for C−H bond scission in *hydroxymethyl*, O−H scission in *hydroxymethyl*, and C−H scission in *hydroxymethylene* on Pt(111). The energy value between the TS and FS images in each elementary step corresponds to the difference in energy between the TS and the products at infinite separation from one another. Further explanatory details are given in the caption of Figure 3.

the extreme right of Figure 5; see also the discussion section for more details). The overall reaction barrier for this step is 0.43 eV, and the energy change is −1.01 eV for conversion to $CO_{(a)} + 2H_{(a)}$ (exothermic step).

The elementary steps corresponding to O−H scission in COH and C−O scission in methanol, together with associated energetic information, are summarized in Figure 6. The CO−H dissociation process begins with an over-top O−H stretch at 3704 cm^{-1} (Table 2) with concomitant tilting of the COH species toward an adjacent platinum atom; the final state has CO adsorbed at an fcc site with H in an hcp site. CH_3-OH scission begins with a C−O stretch at 976 cm^{-1} and ends with CH_3 and OH adsorbed on neighboring top sites. The indicated frequencies become imaginary at the associated transition states.

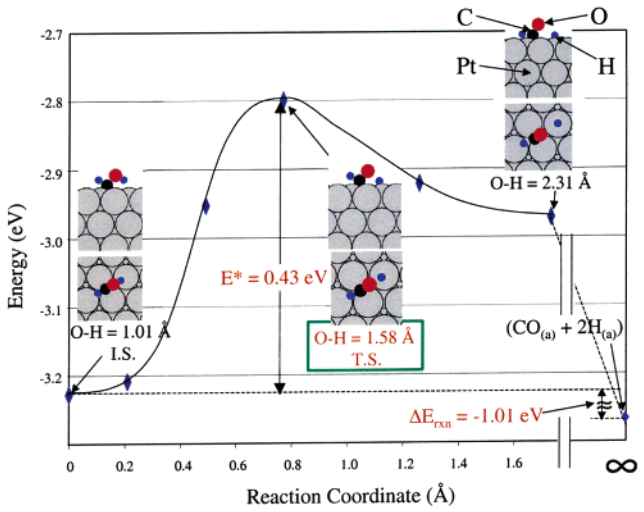

Figure 5. Reaction coordinate for O−H bond scission in *hydroxymethylene* on Pt(111). The energy zero is gas-phase HCOH and a clean Pt(111) slab at infinite separation from one another. Further explanatory details are given in the caption of Figure 3.

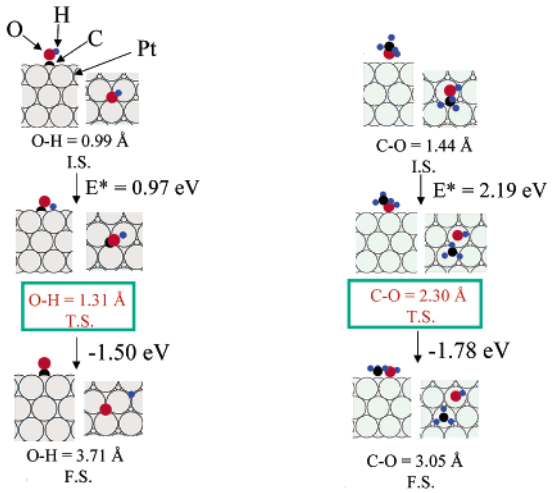

Figure 6. Reaction coordinates for O−H bond scission in *hydroxymethylidyne* and for C−O scission in *methanol* on Pt(111). The energy value between the TS to FS images in each elementary step corresponds to the difference in energy between the TS and the products at infinite separation from one another. Further explanatory details are given in the caption of Figure 3.

Complete Methanol Decomposition Pathway on Pt(111). A detailed, one-dimensional, potential energy surface (PES) for the decomposition of methanol initiated with a C−H bond scission event is presented in Figure 7a. Gas-phase methanol at infinite separation from Pt(111) is shown on the left side of the figure. The thermochemistry and the activation energy barriers of the subsequent hydrogen abstraction steps follow to the right, and gas-phase CO and H_2 are depicted on the extreme right of the figure. For comparison, data from our previous work[10] showing intermediates resulting from the path starting with an O−H bond scission in MeOH are sketched with dotted lines. Figure 7b shows similar data but with zero-point energy corrections included for both the thermochemistry and the activation energy barriers of the various elementary reactions. In Figure 8, an alternative representation of the non-ZPE corrected PES, showing intermediates from both C−H and O−H scission in methanol, is given. The three most probable methanol decomposition pathways are indicated with dashed lines.

Discussion

Thermochemistry, Elementary Decomposition Steps, and Frequencies of Reaction Intermediates. (a) Methanol. Our results for the adsorption of *methanol* on Pt(111) have been described in detail in our previous paper.[10] In the present article, we compare our previous results with other data that have come to our attention since the publication of our last paper, and we briefly describe the vibrational spectra presented for the first time in this work. Desai et al.[13] found that methanol binds through oxygen at a top site on Pt(111), in good agreement with our results. Their calculated O−Pt bond length (2.59 Å) is somewhat longer than the corresponding value in our calculations (2.43 Å), and the binding energy (BE) that they report (∼−0.45 eV) is slightly larger than our BE of −0.33 eV. These discrepancies could be due to the higher coverage used in their calculations (1/4 ML vs 1/9 ML in our work) and to the more pronounced effects of hydrogen bonding at that coverage.

The first calculated vibrational spectrum for methanol in Figure 2a (with two methyl hydrogen atoms pointing toward the Pt(111) surface−see Table 2 for a list of frequencies) is in reasonable agreement with the experimentally measured spectrum, suggesting that the most favorable adsorption configuration that we have described for methanol is generally accurate. The second methanol spectrum in Figure 2a (with a single methyl hydrogen pointing toward the surface) is substantially similar to the first spectrum; it is only the lowest frequency mode that is noticeably different between the two configurations.

Relatively few data exist with which to compare our calculated activation energy barriers for methanol decomposition (0.81 eV for O−H bond scission,[10] 0.67 eV for C−H scission, and 2.19 eV for C−O scission). Molecular beam studies[27] have given an estimate of ∼0.5 eV (with respect to gas-phase methanol) for the barrier for the first step in methanol decomposition on Pt(111). Our lowest calculated barrier (0.67 eV with respect to adsorbed methanol) is ∼0.43 eV with respect to gas-phase methanol (including a 0.09 eV thermochemical barrier necessary to go from the most stable methanol state to the initial state for the C−H scission pathway which is the metastable state described in the results section), in good agreement with the experimental result. Periodic DFT calculations on a 2 × 2 unit cell[13] have determined barriers of 1.47 and 0.95 eV for O−H and C−H scission in methanol, respectively. These values are significantly higher than our values, and the difference between the two barriers is much larger than is the corresponding difference in our work. These deviations may be related to the increased constraints on the transition state geometry that are imposed at the higher coverages used in the cited study.

We are not aware of any experiments on Pt(111) in which C−O bond scission in methanol has been observed (some authors did, however, observe this reaction on (1 × 1)Pt-(110)[28,29]). The lack of experimentally observed C−O bond scission is consistent with our finding of an extremely high activation energy barrier (2.19 eV) for this reaction.

(b) Methoxy. Our results for adsorbed *methoxy* have also been discussed in a previous article.[10] Here, we simply describe

(27) Diekhöhner, L.; Butler, D.; Baurichter, A.; Luntz, A. *Surf. Sci.* **1998**, *409*, 384−391.
(28) Wang, J.; Masel, R. I. *J. Catal.* **1990**, *126*, 519−531.
(29) Wang, J.; Masel, R. *J. Am. Chem. Soc.* **1991**, *113*, 5850−5856.

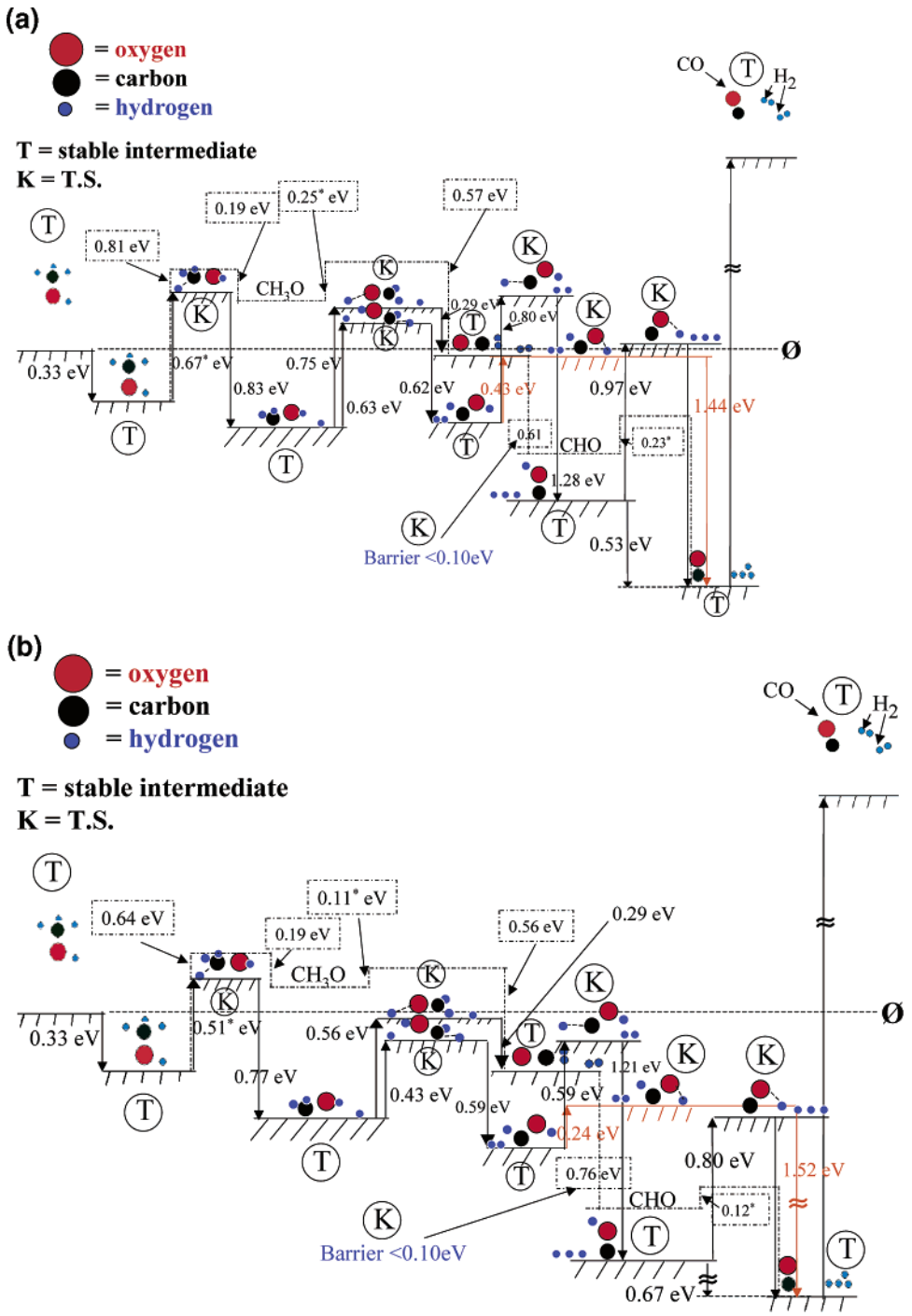

Figure 7. (a) One-dimensional potential energy surface (PES) for methanol decomposition on Pt(111). The dashed lines denote elementary steps resulting from O−H scission in methanol and subsequent dehydrogenation [Greeley et al. *J. Am. Chem. Soc.* **2002**, *124*, 7193]. The solid lines denote all other steps. Molecular schematics correspond only to configurations indicated by solid lines. The symbol "≈" indicates that an energy line is not drawn to scale. Zero-point energies are not included. All adsorbed hydrogen shown in the schematics is atomic H. The pathway indicated in orange is the quasi-concerted decomposition of HCOH described in the text. The indicated activation energy barriers for dehydrogenation reactions are for bond-breaking processes only; the values do not include small diffusion barriers that may need to be overcome for the reactant to move from its most stable state to the initial state for the bond-breaking event. Asterisks indicate that such a diffusion barrier (on the order of 0.1 eV) exists for a particular reaction. (b) One-dimensional PES with zero-point energy effects included for both the stable intermediates and the transition states.

the calculated vibrational spectra presented in Figure 2b, and we compare these spectra to the experimental EELS spectrum of Sexton[30] for methoxy on an oxygen-precovered Pt(111) crystal (also sketched in Figure 2b). The agreement between the experimental spectrum and the simulated spectrum for methoxy in a tilted top configuration is good. The experimental band at 370 cm^{-1} is assigned by Sexton to the O−Pt stretch in methoxy (the O−Pt stretch for atomic oxygen is measured at 470 cm^{-1}); we note, in passing, that Peck et al.[31] have measured

(30) Sexton, B. *Surf. Sci.* **1981**, *102*, 271−281.

(31) Peck, J.; Mahon, D.; Beck, D.; Bansenaur, B.; Koel, B. *Surf. Sci.* **1998**, *410*, 214−227.

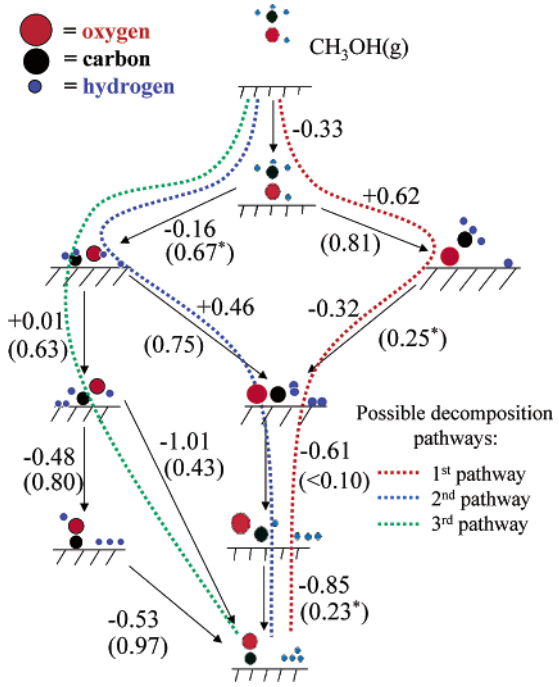

Figure 8. Schematic summary of the reaction network for methanol decomposition through C−H and O−H bond scission in methanol on Pt(111). Values without parentheses are energy changes of the indicated elementary steps (negative values indicate exothermic steps). Values in parentheses are activation energy barriers. The energies do not include zero-point energy corrections. The dotted lines correspond to likely decomposition pathways for methanol, as indicated in the figure legend. The asterisks have the same meaning as in Figure 7.

a band at 310 cm^{-1} that they assign to an O−Pt stretch in deuterated methoxy (CD_3O) on Pt(111), but they caution that the overlayer in their experiments contains many species and that the assignment is not unambiguous. In any case, these experimental frequencies are close to our calculated O−Pt stretch at 431 cm^{-1}. The other calculated modes are also in good agreement with the experimental results (Figure 2b and Table 2).

Perhaps the most significant difference between the two calculated methoxy spectra in Figure 2b is that the spectrum for methoxy in a perpendicular fcc configuration lacks a low-frequency O−Pt stretch mode of high intensity. This fact, combined with the observation that both the experimental spectrum and the simulated spectrum for the tilted top configuration show this mode, strongly suggests that methoxy adsorbs in a tilted top configuration on Pt(111). This conclusion is also supported by our calculated CH_3O/Pt(111) binding energy trends. Additionally, indirect experimental support for this conclusion is provided by somewhat remotely relevant NEXAFS measurements.[32] Those results demonstrate that the C−S bond of thiomethoxy (CH_3S) is inclined at an angle of ∼45° with respect to the surface normal on Pt(111).

(c) Carbon Monoxide. *Carbon monoxide* adsorption was discussed in detail in our recent work,[10] and here we limit our discussion to a comparison of the experimental ($\theta = 0.17$ ML) and calculated ($\theta = 0.11$ ML) frequency spectra (Figure 2c). The experimental peak at 470 cm^{-1} is assigned to a Pt−CO stretch;[33] the calculated Pt−CO stretch on the top site is found at 467 cm^{-1}, in excellent agreement with the experiments. The experimental C−O stretch is found at 2100 cm^{-1}, and the corresponding calculated frequency (top site) is 2137 cm^{-1}. At higher coverages, the experiments show the appearance of two additional modes, one at 380 cm^{-1} and the other at 1850 cm^{-1} (second CO panel of Figure 2c). These modes are assigned to bridge-site CO, but we note that the measured frequencies overlap closely with the calculated frequencies for CO in fcc sites (1822 and 356 cm^{-1}).

Experiments generally show that CO prefers to adsorb at top sites on Pt(111). This conclusion is supported by our simulated vibrational spectra; the calculated spectrum for CO on a top platinum site is in good agreement with experimental results. However, our calculated binding energy for CO is greatest at fcc sites (BE = −1.82 eV). It therefore appears that the simulated vibrational spectra are in agreement with the experimental site preference, but the calculated binding energies are not (the discrepancy between the calculated CO site of lowest energy and the experimental site preference is a common problem with DFT; it is generally attributed to inaccuracies in the GGA treatment of CO adsorption).[34,35] This situation might be explained by postulating that the GGA-calculated CO energies near each adsorption site are shifted by a roughly constant amount from the true energies. This uniform shift would imply that the curvature of the potential energy surface (and thus, the corresponding vibrational frequency) near each site was not significantly changed. The absolute values of the energies might, however, still be off by a considerable (and different) amount at each site, thus leading to the erroneously calculated site preferences.

(d) Hydroxymethyl. The *hydroxymethyl* radical is sufficiently unstable on Pt(111) that, to our knowledge, no experimental structural information has been obtained for this species. However, a few DFT studies of this radical do exist. Periodic slab calculations[13] find that CH_2OH binds through carbon to a top site; the binding energy is −2.17 eV. Cluster calculations find similar adsorption geometries with BEs of −2.51 eV[12] and −2.85 eV.[11] Our calculated adsorption geometry is in agreement with the geometries found in each of these studies. The binding energy from the slab calculation is in reasonable agreement with our value of −1.98 eV, but the BEs from the cluster calculations are significantly higher than our value. This discrepancy could perhaps be due to the finite cluster sizes used in those studies.

Unfortunately, no experimental determinations of the activation energy barrier to hydroxymethyl decomposition through either C−H or O−H scission have been made. An estimate from a previous periodic slab calculation at 1/4 ML coverage[13] does, however, exist for the O−H scission process; the barrier in that study was found to be 1.24 eV. This barrier is significantly higher than the barrier of 0.75 eV found in our study (see also discussion below); the difference may be due to the different coverages used in the respective calculations.

(e) Hydroxymethylene. The *hydroxymethylene* (HCOH) radical is also unstable on Pt(111), and we are not aware of experimental data on the structure or binding strength of this species. A DFT cluster study[12] found that HCOH prefers top site adsorption through the carbon atom (although the authors

(32) Koestner, R. J.; Stöhr, J.; Gland, J. L.; Kollin, E. B.; Sette, F. *Chem. Phys. Lett.* **1985**, *120*, 285−291.
(33) Steininger, H.; Lehwald, S.; Ibach, H. *Surf. Sci.* **1982**, *123*, 264−282.
(34) Feibelman, P.; Hammer, B.; Nørskov, J.; Wagner, F.; Scheffler, M.; Stumpf, R.; Watwe, R.; Dumesic, J. *J. Phys. Chem. B* **2001**, *105*, 4018−4025.
(35) Grinberg, I.; Yourdshahyan, Y.; Rappe, A. M. *J. Chem. Phys.* **2002**, *117*, 2264−2270.

speculate that bridge adsorption may have similar energetics); the binding energy is reported to be −3.79 eV. Another cluster study[11] finds that bridge adsorption is preferred with a BE of −3.68 eV. The reported site preferences in these studies are in good agreement with our calculated preferences (we find that bridge and top sites have comparable energetics) although the indicated binding energies are somewhat higher than our value of −3.24 eV. This discrepancy may be due to the fundamental differences between cluster and slab calculations. No experimental or theoretical data exist to compare to our results for the activation energy barriers to HCOH decomposition.

(f) Hydroxymethylidyne. The final intermediate considered in this discussion is *hydroxymethylidyne* (COH). DFT cluster calculations have yielded binding energies of −4.86 eV[12] and −5.25 eV[11] for this species. These values are somewhat higher than the corresponding value from our calculation (−4.45 eV); the explanation for this difference is likely the same as the explanation postulated above for the discrepancies between the cluster and slab results in CH_2OH and HCOH. Unfortunately, as is the case with the hydroxymethylene species, no data exist to compare with our calculated activation energy barrier for COH decomposition to $CO_{(a)}$ and $H_{(a)}$.

For each of the elementary decomposition steps mentioned above, a single vibrational mode in the reactant of the step in question can be identified as the beginning of the reaction coordinate for that step (see also the Results section). These modes qualitatively resemble the appropriate reaction coordinate (e.g., asymmetric C−H stretches are found to begin C−H scission reactions), and the modes disappear at the transition state.

Reaction Network. (a) Potential Energy Surface for Methanol Decomposition. The potential energy surface in Figure 7a gives both thermochemical data and activation energy barriers for the elementary reaction steps following an initial C−H bond scission in methanol. Possible connections between this pathway and the pathway starting with O−H bond scission in methanol [10] are also shown. The latter pathway itself is sketched with dotted lines. It is immediately seen that adsorbed intermediates from C−H scission in methanol (CH_2OH, HCOH, and COH) are more stable than are the corresponding adsorbed isomers from O−H scission (CH_3O, CH_2O, CHO). Adsorbed hydroxymethyl, for example, is ∼0.8 eV more stable than adsorbed methoxy. Adsorbed hydroxymethylene is ∼0.45 eV more stable than adsorbed formaldehyde, and adsorbed hydroxymethylidyne is ∼0.3 eV more stable than adsorbed formyl. In the absence of activation energy barriers, or at equilibrium conditions, these increased stabilities would ensure that the C−H derived intermediates would be found at higher surface coverages, and the reaction would almost certainly proceed primarily through these intermediates. Such a conclusion would be consistent with the results of Franaszczuk et al.[6] in electrochemical environments and with recent theoretical results on Pd(111).[36] We note, however, that the activation energy barriers of the apparent rate determining steps of the various decomposition pathways are of comparable magnitude, suggesting that multiple pathways might contribute to the overall rate.

(b) Decomposition Pathways. In total, the DFT results suggest that three pathways (Figure 8) may be important in determining the net rate of reaction. The first pathway proceeds as follows: $CH_3OH \rightarrow CH_3O \rightarrow CH_2O \rightarrow HCO \rightarrow CO$. This is simply the O−H scission pathway that has already been described in detail;[10] the rate-limiting step of this pathway is the first step, the abstraction of a hydroxyl hydrogen from methanol. The second pathway involves an initial C−H bond scission in methanol: $CH_3OH \rightarrow CH_2OH \rightarrow CH_2O \rightarrow HCO \rightarrow CO$. According to our results, cleavage of the O−H bond in CH_2OH to produce formaldehyde (CH_2O) would likely be the rate-limiting step of this pathway although the barrier to C−H bond scission in methanol (the first step in the pathway) is of only slightly lesser magnitude. We note that this pathway was analyzed by Desai et al. in their recent publication.[13] The final pathway proceeds as follows: $CH_3OH \rightarrow CH_2OH \rightarrow HCOH \rightarrow CO$. This pathway starts out with C−H scission in methanol. The resulting intermediate undergoes a second C−H scission to produce HCOH. HCOH then decomposes in a quasi-concerted reaction to form CO. This last step begins with O−H scission in HCOH (see the Results section and Figure 5). A configuration resembling adsorbed formyl (HCO) forms, but the C−O bond is tilted at a much higher angle to the surface than is the C−O bond in our previously identified adsorbed formyl species.[10] This pseudo-formyl configuration does not appear to be a stable state. Because of the close proximity of the remaining carbonic hydrogen to the surface, the pseudo-formyl species undergoes spontaneous C−H bond scission to yield CO (we observed this effect with a variety of ionic time steps and different numbers of layers in the platinum slab). This effect appears to be related to the coverage of surface hydrogen; the abstracted hydroxyl hydrogen in HCOH forces the remaining formyl group to rotate away from the abstracted hydrogen. The rotation brings the carbonic hydrogen close to the surface, leading to spontaneous C−H bond scission.

The contribution of each of the above pathways to the net rate of reaction under realistic reaction conditions will likely depend on temperature and pressure. To quantify the effect of these variables, we have constructed a microkinetic model of the reaction network based on our DFT results. Details of the model will be given in a subsequent paper;[37] here, we simply note that the model is able to account for *T* and *P* effects, and it accurately reproduces experimental data for methanol decomposition on supported Pt catalysts. The model demonstrates that the decomposition reaction proceeds relatively rapidly at conditions of modest temperature and pressure (∼150 °C and 1 atm), in contrast to the complete lack of activity for this reaction under UHV conditions.[10] The model also suggests that, for a wide range of reaction conditions, the initial decomposition step involves C−H scission in methanol to produce hydroxymethyl. The net rate of this step is orders of magnitude higher than is the corresponding rate for CH_3O−H scission, both because of the slightly lower activation barrier for C−H scission and because the high barrier of the reverse step prevents any back reaction from occurring (thus increasing the net rate). The second step in the decomposition pathway is C−H scission in CH_2OH, yielding adsorbed CHOH. As was the case with the initial decomposition step, this C−H scission event has a net rate several orders of magnitude higher than the competing O−H scission step (the latter step yields CH_2O). The final step involves CHOH decomposition via the low-barrier, quasi-

(36) Schennach, R.; Eichler, A.; Rendulic, K. D. *J. Phys. Chem. B* **2003**, *107*, 2552−2558.

(37) Kandoi, S.; Greeley, J.; Dumesic, J. A.; Mavrikakis, M., in preparation.

concerted mechanism described above to yield CO, the most abundant surface species ($\theta_{CO} \approx 0.9$ under most conditions).

Adsorbed hydroxymethylidyne (COH) plays the role of a spectator species in the methanol decomposition reaction. Although this species is thermochemically very stable, the barriers to both its formation and its decomposition are high (0.80 and 0.97 eV, respectively). Under typical steady-state reaction conditions, the microkinetic model predicts a modest COH coverage (~0.1), but this species does not appear to have substantial activity for CO formation. Under UHV conditions, it may be that COH does not form at all; the quasi-concerted decomposition of HCOH (described above) provides a low-barrier process (0.43 eV) that completely bypasses the COH intermediate; this pathway would be expected to be favored over COH formation from HCOH. We note that, if COH could be delivered to Pt(111) under UHV conditions through the use of an appropriate precursor, it could be studied in the low coverage limit because of the barrier heights protecting it. Finally, the barrier to C−O bond scission in methanol is prohibitively high (~2.2 eV), and this decomposition pathway will not be important under any conditions.

(c) Other Reactions between Decomposition Intermediates. Although we have focused on dehydrogenation reactions in the present work, we note that direct reactions between the intermediates shown in Figure 7 might be kinetically significant. We have performed preliminary calculations for certain of these direct reactions (e.g., COH + $CH_3O \rightarrow$ CO + MeOH) and have found low barriers; the significance of these additional pathways will be discussed briefly in our microkinetic study.[37] We note that isomerization reactions of any of the intermediates in Figure 7 (e.g., direct conversion of methoxy to hydroxymethyl) are not likely to be kinetically important steps; preliminary data suggest that these intramolecular H-transfer reactions have barriers on the order of 1.2 eV or greater. Finally, we point out that, because of microscopic reversibility, Figure 7 can be used to analyze hydrogenation reactions in addition to the dehydrogenation reactions analyzed above. The figure indicates, for example, that CO hydrogenation proceeds more easily through carbon than through oxygen, a fact that is simply the result of the close proximity of carbon to the Pt(111) surface in adsorbed CO.

(d) Elusive Intermediates. None of the new intermediates introduced in this study have been experimentally observed. The PES in Figure 7a is consistent with this observation. The barriers for decomposition of the O−H scission intermediates are all less than 0.25 eV, indicating that these intermediates will decompose extremely rapidly. The barriers for decomposition of the C−H scission intermediates are generally higher, but trapping is still unlikely. COH, as described above, will probably not form under UHV conditions. HCOH has a significant barrier to decomposition (~0.4 eV), but this barrier is still much less than the corresponding barrier to its formation (0.63 eV), suggesting that the surface coverage of HCOH will be negligibly small. The barrier to decomposition of CH_2OH (0.63 eV) is slightly less than the barrier to its formation through C−H scission in methanol (0.67 eV). In this case, the results suggest that a small amount of CH_2OH might be trapped on Pt(111), in apparent contradiction to the experimental results. However, given the very similar values of the two barriers, the dominant factors determining the CH_2OH coverage will likely be temperature and pressure effects; our microkinetic model, which explicitly accounts for such effects, suggests that the CH_2OH coverage will, in fact, be vanishingly small. Desai et al.,[13] in their higher coverage studies ($\theta/\theta_{sat} \approx 0.69$, based on an estimated saturation coverage of 0.36 ML[38]), find a much greater difference between the formation (0.95 eV) and the decomposition (1.24 eV) barriers of CH_2OH than we do. Their results certainly suggest that CH_2OH could be experimentally trapped on Pt(111); they explain the absence of experimental observations by proposing that the species actually decomposes over steps on Pt(111) crystals. Although a similar argument could be applied to other intermediates as well, these authors suggest that the steps would lower the decomposition barrier of CH_2OH and render it experimentally unobservable. This explanation is reasonable, but our results suggest that, given the comparable formation and decomposition barriers for CH_2OH at the low coverages analyzed in our study, and given temperature and pressure effects, it is also possible that CH_2OH decomposes rapidly on defect-free areas of Pt(111).

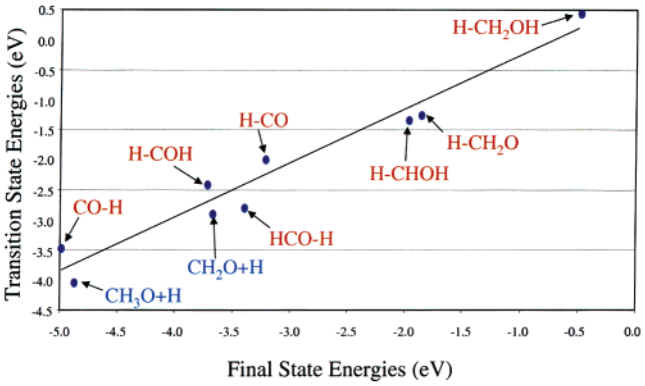

Figure 9. Correlation of transition state energies with final state energies for the elementary steps in methanol decomposition on Pt(111). All elementary steps have been written as exothermic reactions. Transition state and final state energies have been written with respect to the gas-phase energy of the reactants of each elementary step. Reactions indicated in red are bond breaking processes, and reactions in blue are bond formation processes. The equation for the best fit line is $E^{TS} = 0.90E^{FS} + 0.61$.

(e) Zero-Point Energies. A comparison of Figure 7, parts a and b, indicates that zero-point energy effects generally reduce the activation energy barriers for the elementary reactions considered in this study. Since the transition states effectively contain one less degree of vibrational freedom than do the initial states, the TSs are less destabilized by ZPE effects, thereby leading to the indicated reduction in the activation barriers. An additional effect of the ZPEs is to induce a downward shift in the energies of most reaction intermediates and transition states with respect to the energy of gas-phase methanol. Finally, we note that, while the magnitude of the energy shifts induced by the ZPE effects is not negligible, these effects do not appear to alter the qualitative trends in the reaction network described above.

(f) Relationships between Thermochemistry and Kinetics. We close this discussion with a comparison of the transition state and final state energies for each elementary reaction step in the methanol decomposition network on Pt(111) (Figure 9). The energy reference for each step is the clean slab plus gas-phase energy of the reactants of the appropriate step. Following

(38) Akhter, S.; White, J. *Surf. Sci.* **1986**, *167*, 101−126.

the framework suggested by Alcala et al.,[39] the elementary reactions are written as exothermic steps, and the initial and final states are defined accordingly. It is seen that there is, in fact, a reasonable linear correlation between the two quantities ($E^{TS} = 0.90E^{FS} + 0.61$), suggesting that it could be possible to estimate transition state energies from the final state energies. The square of the correlation coefficient (0.95) is close to one, and while the absolute value of the standard error is fairly large (0.31 eV), the relative error (~9%) is reasonably small (we note that writing each step as a hydrogenation reaction gives a comparable correlation, $E^{TS} = 0.92E^{FS} + 0.29$, with a standard error of 0.24 eV). Nonetheless, it is clear that predictions made using the correlation in Figure 9 will be approximate at best, and, depending on the specific situation, it is even possible that the correlation might incorrectly identify the rate-limiting step of a reaction pathway. The derived linear correlation should therefore be used with caution. It is also worth noting that the slope of the best linear fit, as identified in Figure 9, is close to unity, a characteristic shared by other similar, recently developed correlations.[39−41] Finally, we point out that the above results could be interpreted to mean that the transition states of the exothermically written elementary reaction steps may be somewhat product-like in nature.

Conclusions

Periodic, self-consistent (GGA-PW91), DFT calculations have been used to study the thermochemistry and reaction barriers of the elementary steps leading to methanol decomposition on Pt(111). Decomposition through reaction pathways beginning with C−H and C−O bond scission in methanol have been analyzed, thus completing the picture of methanol chemistry begun in an earlier paper.[10] DFT results suggest that the decomposition reaction may proceed through any of three pathways: (i) O−H bond scission in methanol followed by sequential dehydrogenation to CO, (ii) C−H bond scission in methanol followed by O−H scission to give formaldehyde and sequential dehydrogenation to CO, and (iii) C−H scission in methanol followed by a second C−H scission and a quasi-simulteneous O−H/C−H scission to CO. A microkinetic model that incorporates the DFT data indicates that the third of these pathways is likely to be dominant under typical reaction conditions. Additionally, the thermochemistry and kinetics of all elementary steps in the reaction network are found to be linearly correlated. Finally, simulated specular HREELS spectra agree well with available experimental spectra and offer vibrational fingerprints of elusive reaction intermediates.

Acknowledgment. J.G. acknowledges partial financial support from a National Science Foundation predoctoral fellowship. This work was supported through an NSF-CAREER Award (CTS-0134561) and a DOE-BES Catalysis Science Grant (DE-FG02-03ER15469). We used resources of the National Energy Research Scientific Computing Center, which is supported by the Office of Science of the U.S. Department of Energy under Contract No. DE-AC03-76SF00098. Both authors acknowledge partial support from NSF cooperative agreement ACI-9619020 through computing resources provided by the National Partnership for Advanced Computational Infrastructure (NPACI). We thank Andrzej Wieckowski, Eric Stuve, Matthew Neurock, Shampa Kandoi, and Jim Dumesic for fruitful discussions.

JA037700Z

(39) Alcala, R.; Mavrikakis, M.; Dumesic, J. D. *J. Catal.* **2003**, *218*, 178−190.
(40) Michaelides, A.; Liu, Z. P.; Zhang, C. J.; Alavi, A.; King, D. A.; Hu, P. *J. Am. Chem. Soc.* **2003**, *125*, 3704−3705.
(41) Nørskov, J. K.; Bligaard, T.; Logadottir, A.; Bahn, S.; Hansen, L. B.; Bollinger, M.; Bengaard, H.; Hammer, B.; Šljivančanin, Z.; Mavrikakis, M.; Xu, Y.; Dahl, S.; Jacobsen, C. J. H. *J. Catal.* **2002**, *209*, 275.